PHYSICAL REVIEW D VOLUME 25, NUMBER 1 1 JANUARY 1982

Central and diffractive components of charm production

V. Barger and F. Halzen
Physics Department, Univeristy of Wisconsin—Madison, Madison, Wisconsin 53706

W. Y. Keung
Brookhaven National Laboratory, Upton, New York 11973

(Received 8 June 1981)

To $O(\alpha_s^2)$ in perturbative QCD one can identify two separate components in the production of heavy flavors such as charm: central $q\bar{q}\to c\bar{c}$, $gg\to c\bar{c}$ and diffractive $qc\to qc$, $gc\to gc$. For diffractive production, QCD evolution is the source of charm quarks inside the colliding hadrons. With an estimated 0.5% charm momentum fraction at $Q^2\simeq 4m_c^2$ from QCD evolution, a hard x distribution of charm, and a resolution cutoff on gluon-exchange contributions, the diffractive component reproduces the Λ_c^+ and D cross sections observed at intermediate to large longitudinal x, both at Fermilab and at CERN ISR energies. The diffractive component also contributes to charm production near $x_L=0$. This explains the failures of previous analyses, based on annihilation diagrams alone, to account for the observed charm cross sections in the central region. Estimates are made of cross sections and x_L dependences of b- and t-quark production up to $\bar{p}p$ collider energies.

I. INTRODUCTION

Two years after the discovery of forward production of charmed particles, the mechanism for the unexpectedly large observed cross sections remains a mystery.[1-3] This is unfortunate for the following reasons.

(i) The large diffractive charm cross sections might be an indication that the forward longitudinal-x region is the best place to search for the production of heavier flavors such as b and t. This question is relevant not only for present experiments, but also for the ongoing design of detectors for future hadron colliders. In the absence of a dynamical scheme that can accommodate the charm data, reliable estimates of the dependence of diffractive production on the quark mass or the energy of the collision cannot be made.

(ii) In the absence of a quantitative understanding of the diffractive component of charm production, it is impossible to make meaningful comparisons of the data on central production of heavy quarks with perturbative calculations of fusion diagrams in quantum chromodyamics (QCD).

In this paper we demonstrate that in fact both the central and diffractive components of charm production can be understood[4] in the context of perturbative QCD. The relevant order-α_s^2 diagrams for the production of charm quarks in hadron collisions are shown in Fig. 1. For diagrams where the heavy-quark pair is produced via two momentum fractions x_1, x_2 carried by light quarks [Fig. 1(a)] or by gluons [Fig. 1(b)], the longitudinal momentum x_L carried by the heavy quark is small. These annihilation graphs contribute to central production (i.e., small x_L) of charm and have been extensively studied. The additional flavor-excitation diagrams in Fig. 1c have been forgotten since early considerations.[5] These graphs account for diffractive production of heavy flavors, such as the production of Λ_c^+ at large x_L in pp collisions.[2,6]

The calculation, described in Sec. II, follows the standard approach of any leading-order perturbative QCD calculation. The essential input is a hard x dependence[7] of the QCD-evolved charm distribution $c(x,\langle Q^2\rangle)$ at $\langle Q^2\rangle\simeq 4m_c^2$, required for evaluation of the diffractive diagrams of Fig. 1(c), and a resolution cutoff on the momentum transfer in gluon-exchange diagrams. In Sec. III we compare the results with data. With the charm input motivated in Sec. II, the calculation repro-

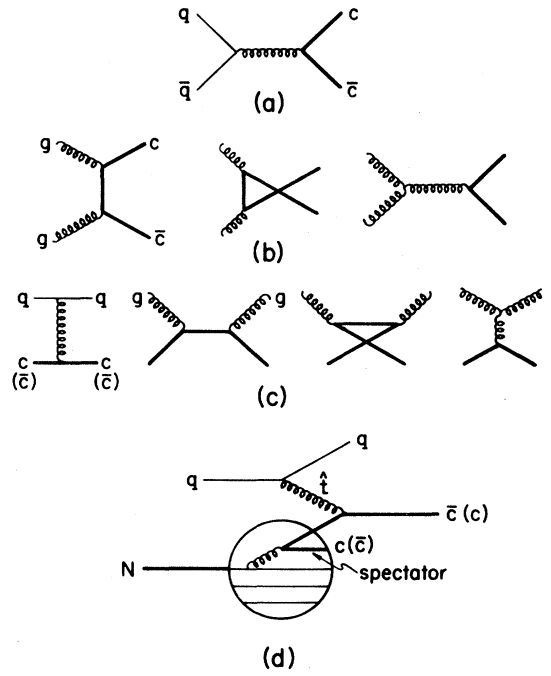

FIG. 1. Order-α_s^2 diagrams for charm production. In part (d) the circle represents a nonperturbative QCD origin of the $c\bar{c}$ in the incident nucleon.

duces the observed levels of charm production in the large-x_L region, e.g., forward Λ_c^+ production at the CERN ISR[6] and diffractive production of $D^{\pm}$ states in $\pi^- p$ collisions at Fermilab.[8] In the central region $x_L \simeq 0$ *both* annihilation and flavor-excitation diagrams contribute to the charm yield. The inability[1] of previous calculations, based on the annihilation diagrams of Figs. 1(a) and 1(b) only, to account for the observed charm cross sections even in the central region was due to the neglect of the diffractive production mechanism of Fig. 1c.

In a final section IV we compute the cross sections for heavier flavors b,t and make projections of the yields and phase-space structure of heavy quarks at energies relevant to the hadron colliders presently under construction.

II. PERTURBATIVE QCD CALCULATION

The cross section σ for the production of heavy quarks in hadron collisions is expressed in terms of the interaction cross section $\hat{\sigma}$ of the constituents as

$$\sigma = \int\int dx_1 dx_2 f_1(x_1,Q^2) f_2(x_2,Q^2) \hat{\sigma} \ , \tag{1}$$

where x_1,x_2 are the momentum fractions carried by the interacting constituents from hadrons 1, 2 and $f_1(x_1,Q^2)$, $f_2(x_2,Q^2)$ specify the probability distributions of these constituents in the initial hadrons. The invariant energy squared s of the hadronic process and that of the constituent subprocess, $\hat{s}$, are related by $\hat{s}=x_1x_2s+{m_1}^2+{m_2}^2$ where m_1,m_2 are the masses of the incoming constituents. The domain of integration in Eq. (1) is $0 \le x_1 \le 1$, $0 \le x_2 \le 1$, $x_1x_2 \ge \hat{s}_o/s$, where $\hat{s}_o=\hat{s}_{\rm th}-{m_1}^2-{m_2}^2$ with $\hat{s}_{\rm th}$ the threshold energy squared. A sum must be made in Eq. (1) over the subprocesses corresponding to the diagrams of Figs. 1a-1c.

The differential cross sections with respect to the longitudinal scaling variable $x_L=2p_L/\sqrt{s}$ of the *scattered* heavy quark can be expressed in terms of $d\hat{\sigma}/d\hat{t}$, where $\hat{t}$ is the subprocess invariant momentum transfer squared, as

$$\frac{d\sigma}{dx_L} = \int\int dx_1 dx_2 f_1(x_1,Q^2) f_2(x_2,Q^2) \times \left[\frac{x_1x_2s}{x_1+x_2}\right] \frac{d\hat{\sigma}}{d\hat{t}} \ . \tag{2}$$

The relation of $\hat{t}$ to the integration variables is

$$\hat{t} = \left[-s(x_1-x_L) + \frac{{m_1}^2+{m_3}^2}{x_1} + \frac{{m_4}^2-{m_2}^2}{x_2}\right] \times \frac{x_1x_2}{x_1+x_2}$$

with m_3,m_4 the masses of the outgoing constituents. The domain of the x_1,x_2 integration is further constrained by the allowed region for $\hat{t}$, discussed below. Under the assumption that the heavy-quark spectator carries the momentum of the proton not carried by the interacting quark, the differential cross section with respect to the fractional longitudinal momentum x_L of the *spectator* heavy quark is

$$\frac{d\sigma}{dx_L} = f_1(x_1,Q^2) \int dx_2 f_2(x_2,Q^2) \hat{\sigma} \tag{3}$$

with $x_1=1-x_L$ and x_2 integration range $\hat{s}_0/(x_1s) \le x_2 \le 1$.

In mapping the kinematic range of $\hat{t}$, it is convenient to introduce the notation

$$x_0=(1-4m^2/\hat{s})^{1/2}\ ,$$
$$y_0=(\hat{s}-m^2)^2/\hat{s}\ , \tag{4}$$

where m is the mass of the heavy quark in Fig. 1. For the fusion subprocesses of Figs. 1(a) and 1(b),

$$m^2-\hat{s}(1-x_0)/2\le-\hat{t}\le m^2+\hat{s}(1-x_0)/2\ , \tag{5}$$

and for the flavor-excitation processes of Fig. 1(c),

$$\hat{t}_{\min}\le-\hat{t}\le\hat{t}_0\ , \tag{6}$$

where

$$\hat{t}_0=\min\{\hat{s}-m^2-\hat{t}_{\min},y_0\}\ . \tag{7}$$

The quantity $\hat{t}_{\min}$ is a cutoff of dynamical origin in QCD that eliminates divergences at $\hat{t}=0$ of gluon-exchange diagrams; we return to further discussion of this point below. Similarly, a cutoff $m^2-\hat{u}>\hat{t}_{\min}$ is imposed on the $\hat{u}$-channel pole diagram.[5]

We now list the expressions for $d\hat{\sigma}/d\hat{t}$ for the subprocesses of Fig. 1 in terms of their Mandelstam invariants $\hat{s},\hat{t},\hat{u}$ and the cross-section factor

$$\hat{\sigma}_0=4\pi\alpha_s^2/(3\hat{s})\ , \tag{8}$$

where α_s is the strong coupling constant at scale Q^2:

$$\frac{d\hat{\sigma}}{d\hat{t}}(q\bar{q}\to Q\bar{Q})=\frac{\hat{\sigma}_0}{3\hat{s}}F(\hat{s},\hat{t},\hat{u})\ , \tag{9a}$$
$$\frac{d\hat{\sigma}}{d\hat{t}}(gg\to Q\bar{Q})=\frac{3\hat{\sigma}_0}{64\hat{s}}G(\hat{s},\hat{t},\hat{u})\ , \tag{9b}$$
$$\frac{d\sigma}{d\hat{t}}(qQ\to qQ)=\frac{\hat{\sigma}_0}{3y_0}F(\hat{t},\hat{s},\hat{u})\ , \tag{9c}$$
$$\frac{d\sigma}{d\hat{t}}(gQ\to gQ)=-\frac{\hat{\sigma}_0}{8y_0}G(\hat{t},\hat{s},\hat{u})\ . \tag{9d}$$

The quantities F and G are defined as

$$F(a,b,c)=[(m^2-b)+(m^2-c)-2m^2a]/a^2\ ,$$
$$G(a,b,c)=\frac{12(m^2-b)(m^2-c)}{a^2}-\frac{2}{3}\frac{m^2(a-4m^2)}{(m^2-b)(m^2-c)}$$
$$+\left\{\left[\frac{8}{3}\frac{(m^2-b)(m^2-c)-2m^2(m^2+b)}{(m^2-b)^2}-6\frac{(m^2-b)(m^2-c)+m^2(c-b)}{a(m^2-b)}\right]+[b\leftrightarrow c]\right\}\ . \tag{10}$$

The integrated subprocess cross sections and their thresholds $\hat{s}_{\rm th}$ are given by[5]

$$\hat{\sigma}(q\bar{q}\to Q\bar{Q})=\hat{\sigma}_0\frac{2x_0}{9}\left[1+\frac{2m^2}{\hat{s}}\right]\ ,\quad \hat{s}_{\rm th}=4M^2\ , \tag{11a}$$
$$\hat{\sigma}(gg\to Q\bar{Q})=\frac{\hat{\sigma}_0}{4}\left[1+\frac{4m^2}{\hat{s}}+\frac{m^4}{\hat{s}^2}\right]\ln\left[\frac{1+x_0}{1-x_0}\right]-\frac{\hat{\sigma}_0x_0}{16}\left[7+\frac{31m^2}{\hat{s}}\right],\quad \hat{s}_{\rm th}=4M^2\ , \tag{11b}$$
$$\hat{\sigma}(qQ\to qQ)=\frac{\hat{\sigma}_0}{3}\left[\left[1-\frac{\hat{t}_{\min}}{y_0}\right]\left[1+\frac{2\hat{s}}{\hat{t}_{\min}}\right]-\frac{2\hat{s}}{y_0}\ln\left[\frac{y_0}{\hat{t}_{\rm mun}}\right]\right],$$
$$\hat{s}_{\rm th}=m^2+\tfrac{1}{2}\hat{t}_{\min}+(m^2\hat{t}_{\min}+\tfrac{1}{4}\hat{t}_{\min}^2)^{1/2}\ , \tag{11c}$$

$$\hat{\sigma}(gc\to gc)=\frac{3\hat{\sigma}_0}{4y_0}\left\{\left[1+\frac{4\hat{s}}{9y_0}\left[1+\frac{m^2}{\hat{s}}\right]^2-\frac{2}{9}\frac{(\hat{t}_0+\hat{t}_{\min})}{(\hat{s}-m^2)}+\frac{2\hat{s}y_0}{\hat{t}_0\hat{t}_{\min}}\right.\right.$$
$$+\frac{16}{9}\frac{m^4}{(\hat{s}-m^2-\hat{t}_0)(\hat{s}-m^2-\hat{t}_{\min})}\left](\hat{t}_0-\hat{t}_{\min})+2(\hat{s}+m^2)\ln\frac{\hat{t}_{\min}}{\hat{t}_0}\right.$$
$$\left.+\frac{4}{9}\frac{(\hat{s}^2-6m^2\hat{s}+6m^4)}{(\hat{s}-m^2)}\ln\frac{\hat{s}-m^2-\hat{t}_{\min}}{\hat{s}-m^2-\hat{t}_0}\right\},\quad \hat{s}_{\rm th}=m^2+2\hat{t}_{\min}\ . \tag{11d}$$

For the fusion processes of Eqs. (11a) and (11b), we assume that the interval $4m^2 \leq \hat{s} \leq 4M^2$ yields bound $Q\bar{Q}$ and that $\hat{s} \geq 4M^2$ corresponds to open heavy flavor production (M is the mass of the lightest meson with flavor Q). The flavor-excitation subprocesses do not contribute to bound $Q\bar{Q}$ production.

The Q^2 scale enters through the momentum distributions $f_1(x_1,Q^2)$, $f_2(x_2,Q^2)$ and the strong coupling constant $\alpha_s(Q^2) = 12\pi/[(33-2f)\ln(Q^2/\Lambda^2)]$. We take an effective Q^2 scale of $4m^2$ and make typical choices $\Lambda = 0.5$ GeV with $f = 4,5,6$ for c,b,t production. All our calculations are based on a gluon distribution[1] $G(x) = 3(1-x)^5/x$ and the light-quark distributions of Owens-Reya[9] evaluated at $Q^2 = 4m^2$. For quark masses we take $m_c = 1.5$, $m_b = 4.7$, and $m_t = 20$ GeV. For the physical thresholds of open heavy flavor production via the fusion mechanisms, we use $M_D = 1.87$, $M_B = 5.24$, and $M_T = 23.3$ GeV.

We next consider the input for the charm distribution $c(x,Q^2)$ which initiates the diffractive diagrams of Fig. 1(c). We hypothesize that the charm or anticharm quarks with which the gluons interact in Fig. 1(c) are not "intrinsic"[7] but are generated by QCD evolution of the structure functions, as illustrated pictorially in Fig. 1(d). That is, we suppose that at low Q^2 the charm content of the proton is virtually nil, but at Q^2 of order $4m_c^2$ one has sufficient resolution to find charm quarks deep inside the proton. The typical flavor-excitation diagram of Fig. 1(d) is analogous to electroproduction if we replace the gluon carrying momentum transfer $\hat{t}$ by a photon with $Q^2 = -\hat{t}$. In deep-inelastic electron scattering the virtual photon must have $Q^2 > Q_0^2$ to excite charm. Similarly, in the gluoproduction diagram of Fig. 1(c), the gluon must carry sufficient momentum transfer squared $\hat{t}$ to ensure that $Q^2 > Q_0^2$. This implies a minimum dynamical resolution $\hat{t}_{\min}$ for the momentum transfer $\hat{t}$ of the $qc \to qc$ and $gc \to gc$ subprocesses in Fig. 1(c), whose amplitudes would otherwise be divergent at $\hat{t} = 0$. A momentum transfer squared of at least $\hat{t}_{\min} = O(m^2)$ is therefore necessary to excite a $c\bar{c}$ pair. We choose $\hat{t}_{\min} = m^2$, although, as in any leading-order QCD calculation, the specification of the scale is uncertain by factors, i,e,, $\hat{t}_{\min} = 4m^2, \frac{1}{4}m^2, \ldots$ are equivalent choices in leading order.

It is usually thought that a charm distribution generated by QCD evolution would be soft. This bias is, however, based on leading-order perturbative QCD and is not relevant to our considerations We are talking about the evolution of the charm distribution from low Q^2 up to $Q^2 \sim 4m_c^2$. In this region the evolution will be rapid, because of the large effective coupling, and any considerations based on perturbation theory are probably irrelevant. Hence it is not incompatible with the spirit of QCD evolution to suppose that the fractional momentum distribution $xc(x,Q^2)$ of charm at $Q^2 \sim 4m_c^2$ will actually be quite hard. [Of course, at higher Q^2, after further (perturbative) evolution, $xc(x,Q^2)$ will peak towards low x, but this is not the kinetic region of interest.]

We are motivated to assume this by the following argument used in other contexts.[7,10] If a $c\bar{c}$ pair is produced and remains bound to the rest of the proton for some time, then the charm quarks must travel with roughly the same velocity as the valence quarks. In this configuration most of the momentum of the proton is carried by charm due to its large mass. Now, this argument relies on having a long time scale. However, for Q^2 less than $4m_c^2$, the time scales are relatively long, so we feel that this argument should have some validity for the early stages of the evolution of the charm distribution. Consequently, we shall assume a charm distribution resembling the broad Bjorken-x distribution of the valence quarks. The difference from the intrinsic-charm picture[7] is that the charm is not present at very low Q^2.

For an explicit evaluation of the flavor-excitation cross section, we assume a QCD-evolved charm distribution of the form

$$xc(x,\langle Q^2\rangle) = Nx^l(1-x)^k \tag{12}$$

at an effective value $\langle Q^2\rangle$ for the processes. The normalization N is fixed such that

$$\int dx\, xc(x) = 0.005 \tag{13}$$

which is the level of charm found at $Q^2 \simeq 4m_c^2$ in the QCD moment analysis of Buras and Gaemers.[11] This choice for N is not crucial, since the normalization of the flavor-excitation cross section is also very dependent on the resolution cutoff $\hat{t}_c$. The parameters l,k are chosen $\geq \frac{1}{2}$ so that $xc(x)$ resembles the momentum distribution of valence quarks. Similar results are obtained with l,k choices that have $l,k \simeq 3$.

III. COMPARISONS WITH DATA

Inclusive charm results for $d\sigma/dx_L$, based on the calculation described in Sec. II, are shown in

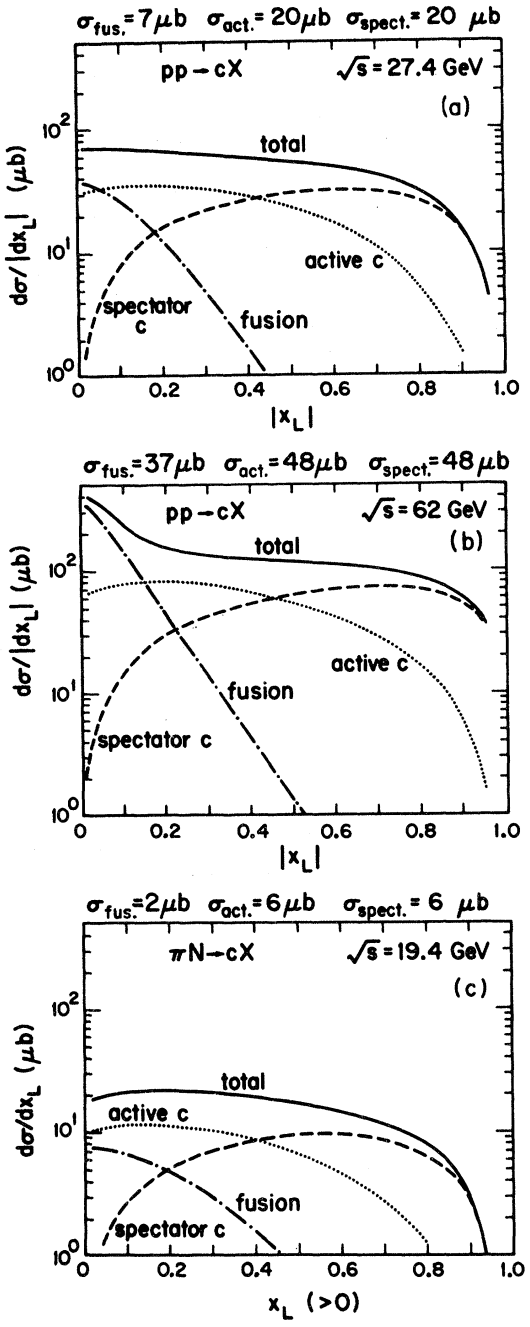

FIG. 2. Longitudinal-momentum distributions for charm excitation in (a) $pp \to cX$ at $\sqrt{s} = 27.4$ GeV, (b) $pp \to cx$ at $\sqrt{s} = 62$ GeV, and (c) $\pi N \to cX$ at $\sqrt{s} = 19.4$ GeV.

Fig. 2 for pp collisions at $\sqrt{2} = 27.4$ and 62 GeV and $\pi^- N$ collisions at $\sqrt{s} = 19.4$ GeV. Also shown separately are the contributions from the fusion diagrams of Figs. 1(a) and 1(b) (the central component) and the contributions of the interacting (active) and spectator c quark from the flavor-excitation diagrams of Fig. 1(c) (the diffractive components). With our choice of the charm distribution $c(x)$, the average x_L of the active c quark is intermediate between that of the centrally produced (average x_L near 0) and spectator (average x_L near 1) c quarks.

Following the scattering subprocess, the charm quarks fragment into charmed hadrons. The spectator charm quark can easily recombine with two parallel moving valence quarks of comparable momentum and thus will fragment primarily into a charm baryon, resulting in Λ_c^+ production at large x_L. The interacting charm quark leads to production at relatively lower x_L of D (or Λ_c^+). Thus diffractive Λ_c^+ data should be compared primarily with the spectator-c component. The forward Λ_c^+ data[6,12] at $\sqrt{s} = 62$ GeV are reproduced by the calculation, as shown in Fig. 3. The ISR measurements and upper bounds on D production[2,6,12] are also plotted in Fig. 3, for comparison with the predictions.

More generally, in pp collisions, we expect the following fragmentation products to be dominant:

spectator c: Λ_c^+ ,

active c: D^+, D^0 ,

active $\bar{c}$: $D^-, \bar{D}^0$,

spectator $\bar{c}$: $D^-, 2\bar{D}^0$.

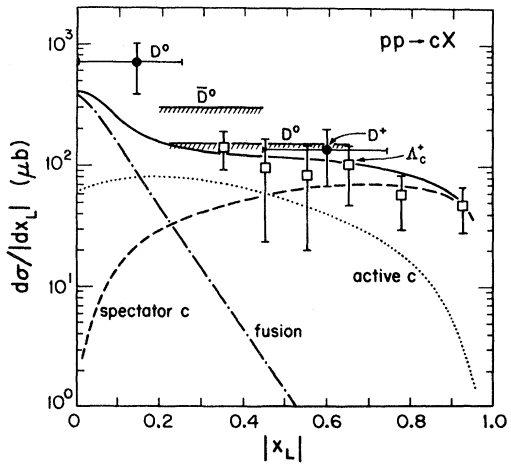

FIG. 3. Results for longitudinal distributions of charm production in $pp \to cX$ at $\sqrt{s} = 62$ GeV compared with ISR data on Λ_c^+ and D production from Refs. 2, 6, and 12.

Comparisons of absolute cross sections can at best be qualitative at the present time, since the data have sizeable systematic and statistical errors and inadequate knowledge of decay branching fractions makes it difficult to translate yields into production cross sections. In view of this, we do not attempt a detailed description of the fragmentation or attempt a best determination of the parameters l,k in Eq. (12) or of the scale $\hat{t}_{\min}$. Further work along these lines can be carried out when the data become more precise.

In Fig. 2(a) we note that in pp collisions the central region at $\sqrt{s}=27.4$ GeV is comparably populated by centrally produced and active c quarks. The predicted yield of 7 μb from the fusion component is below that of present observations. The pp charm-production experiments at $\sqrt{s}\sim 27$ GeV suggest that the central-production cross section is of order 20 μb, with a factor-of-2 uncertainty. An additional ~ 20 μb from the active-c-quark process bridges the gap with the data on D production at this $\sqrt{s}$.

The Princeton-Saclay-Torino-BNL group[13] reported a $\pi^- N$ cross section $d\sigma/dx_L=10$ μb for D^* at $x_L=0$ and $\sqrt{s}=19.4$ GeV. Assuming that $\sigma_{D^*}\simeq\sigma_D$, this agrees with the 20 μb prediction at $x_L=0$ of Fig. 2(c). Even more interesting is that, unlike QCD calculations of fusion processes alone, we obtain a diffractive yield at $\sqrt{s}\sim 20$ GeV of $\sigma\sim 10$ μb over the intermediate x_L range covered by the Illinois-Fermilab-Harvard-Oxford-Tufts $\pi^- p$ experiment,[8] in accord with the observed cross section. Their result that $\sigma_{D^+}\simeq\sigma_{D^-}$ agrees with our expectation based on the dominant role of the active c and $\bar{c}$ quarks in this x_L range. In the forward region $x_L\gtrsim 0.7$, where the spectator quark is dominant, the leading fragmentation products of the π^- should be D^-,D^0.

The dependence of the diffractive charm cross section [i.e., flavor excitation via the diagrams of Fig. 1(c)] is shown versus $\hat{t}_{\min}$ at $\sqrt{s}=62$ GeV in Fig. 4(a). For $\hat{t}_{\min}$ in the range $m_c{}^2$ to $4m_c{}^2$, the diffractive crosss section varies from 100 to 10 μb. This range of cross-section values is in agreement with ISR experimental indications. The spectator and active c quarks contribute equally to σ so the Λ_c^+ cross section is expected to be at least $\frac{1}{2}$ of the total diffractive cross section (due to the fragmentation of the spectator c quark to Λ_c^+).

To estimate diffractive b-quark production, we change the heavy-quark mass to $m_b=4.7$ GeV, take $\langle Q^2\rangle\simeq 4m_b{}^2$, and change the physical cutoff to

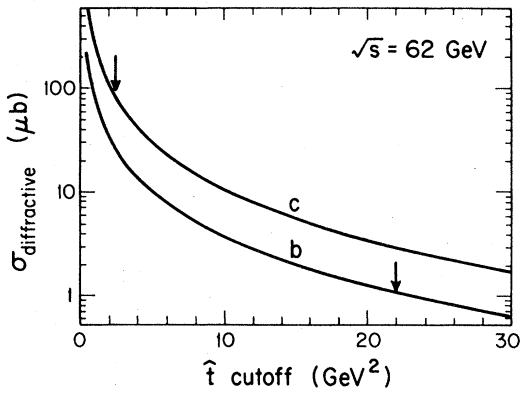

FIG. 4. Total c and b diffractive cross sections [diagrams of Fig. 1(c)] at $\sqrt{s}=62$ GeV versus the QCD dynamical cutoff $\hat{t}_{\min}$ on the subprocess momentum transfer $\hat{t}$. The cutoff values $m_c{}^2$ and $m_b{}^2$ are denoted by arrows.

$$(\hat{t}_b)_{\min}=\frac{m_b{}^2}{m_c{}^2}(\hat{t}_c)_{\min}\ . \tag{14}$$

This cutoff reflects the excitation necessary to produce a $b\bar{b}$ pair in the company of the usual constituents of the nucleon. We further assume that the evolved $xb(x,\langle Q^2\rangle)$ distribution at the appropriate $\langle Q^2\rangle$ for b production is similar to that used in the charm analysis. The resulting b-production cross sections are shown in Fig. 4(b) versus $(\hat{t}_b)_{\min}$. We estimate that the Λ_b^0 cross section at $\sqrt{s}=62$ GeV is at the few-percent level of the Λ_c^+ cross section for $(\hat{t}_b)_{\min}$ given by Eq. (14).

The transverse-momentum distribution of the spectator fragments is expected to be comparable to that of light-quarks fragments, $\langle p_T\rangle\simeq 0.3$ Gev, though it may be somewhat larger due to the increased mass. The interacting charm quark is produced with $p_T{}^2\simeq Q^2$, which results in a broadening of the p_T distribution, in qualitative accord with observations.[6]

The forward Λ_c^+ production via a spectator quark occurs with an accompanying short-distance interaction. Therefore we expect the nuclear dependence to be A^1, as for central production, and not $A^{2/3}$, which might have been expected otherwise.

We conclude this section by pointing out that $c(x,Q^2)$ is expected to fall at large fixed x with increasing Q^2. The stringent experimental limits[14] on $c(x,Q^2)$ from charm-muoproduction data at high Q^2 pose therfore no difficulty here, unlike the case for instrinsic charm.

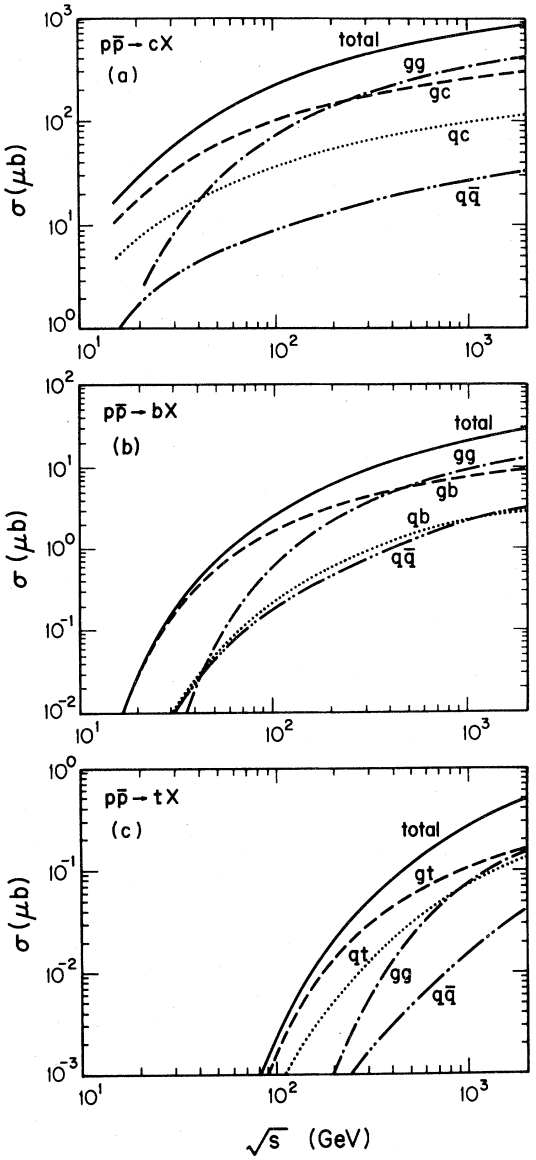

FIG. 5. Energy dependences of heavy-quark cross sections (a) $p\bar{p}\to cX$, (b) $p\bar{p}\to bX$, (c) $p\bar{p}\to tX$ with $m_t=20$ GeV.

IV. PREDICTIONS FOR FUTURE COLLIDER ENERGIES

Although our estimates involve quantitative uncertainties, it nevertheless seems plausible that diffractive production of charm is understandable in perturbative QCD. The QCD calculation can therefore be used to estimate cross sections for heavy-flavor production when the collision energy $\sqrt{s}$ or the quark mass are increased. The energy

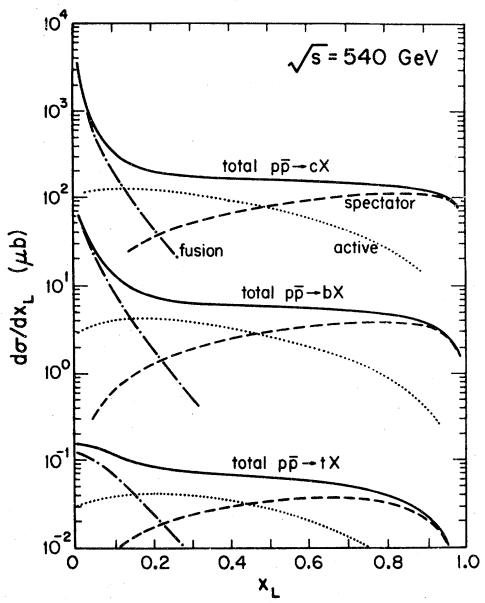

FIG. 6. Longitudinal-momentum distributions of heavy-quark production at $\sqrt{s}=540$ GeV (a) $p\bar{p}\to cX$, (b) $p\bar{p}\to bX$, (c) $p\bar{p}\to tX$ with $m_t=20$ GeV.

dependences of the components of the charm cross section are shown in Fig. 5(a). At 2 TeV, the total charm-production cross section is about 1 μb, in agreement with cosmic-ray observations.[3] The $\sqrt{s}$ dependence of the b- and t-quark (with $m_t=20$

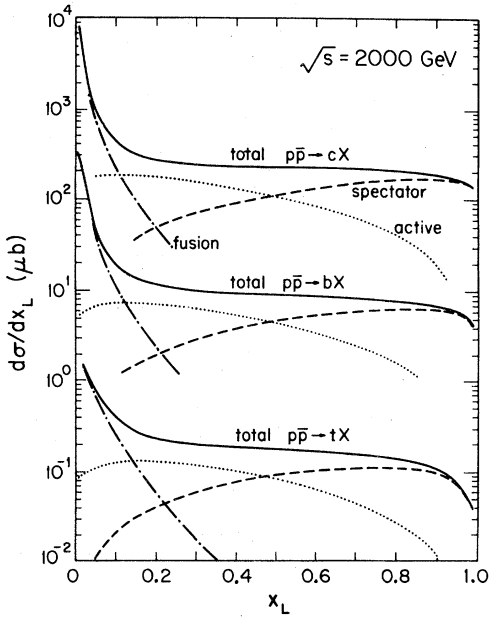

FIG. 7. $d\sigma/dx_L$ at $\sqrt{s}=2000$ GeV. (a) $p\bar{p}\to cX$, (b) $p\bar{p}\to bX$, (c) $p\bar{p}\to tX$.

GeV) cross sections are given in Fig. 5(b), and 5(c). The $d\sigma/dx_L$ dependences of c, b, and t production are shown in Fig. 6 at $\sqrt{s}=540$ GeV (CERN collider) and in Fig. 7 at $\sqrt{s}=2000$ GeV (Fermilab collider).

An important conclusion can be derived from these calculations, which is unlikely to depend on any quantitative uncertainties: at collider energies the proportion of diffractive production is higher for heavy quarks $(t,\ldots)$ than for the lighter (b,c) quarks which are produced predominantly in the central region. The threshold behavior is such that the diffractive component dominates at low energies and the central component dominates at high energies; the energy at which this crossover occurs depends on the quark mass. For the t-quark mass this crossover is still not reached at future collider energies.

ACKNOWLEDGMENTS

We thank R. J. N. Phillips and P. Stevenson for discussion. This research was supported in part by the University of Wisconsin Research Committee with funds granted by the Wisconsin Alumni Research Foundation, and in part by the Department of Energy under Contracts Nos. DE-AC02 76ER00881-215 and 76CH00016.

[1]For a review, see R. J. N. Phillips, in *High Energy Physics — 1980* proceedings of the XXth International Conference, Madison Wisconsin, edited by L. Durand and L. G. Pondrom (AIP, New York, 1981), p. 1470.

[2]An excellent summary of the data on charm production is given by S. Wojcicki, in *High Energy Physics — 1980* (Ref. 1), p. 1430.

[3]F. Halzen, in *Cosmic Rays and Particle Physics — 1978,* proceedings of the Bartol Conference, edited by T. K. Gaisser (AIP, New York, 1979), p. 261.

[4]V. Barger, F. Halzen, and W. Y. Keung, Phys. Rev. D 24, 1428 (1981).

[5]B. L. Combridge, Nucl. Phys. B151, 429 (1979). In this paper no forward production of charm was obtained due to the assumption of a soft charm distribution.

[6]M. Basile *et al.*, Lett. Nuovo Cimento 30, 481 (1981); 30, 487 (1981).

[7]S. J. Brodsky, P. Hoyer, C. Peterson, and N. Sakai, Phys. Lett. 93B, 451 (1980); S. J. Brodsky, C. Peterson, and N. Sakai, Phys. Rev. D 23, 2745 (1981).

[8]L. J. Koester *et al.*, in *High Energy Physics — 1980* (Ref. 1), p. 190.

[9]J. F. Owens and E. Reya, Phys. Rev. D 17, 3003 (1978).

[10]M. Suzuki, Phys. Lett. 68B, 164 (1977); J. D. Bjorken, Phys. Rev. D 17, 171 (1978); C. T. Day and M. Suzuki, *ibid.* 23, 1951 (1981).

[11]A. J. Buras and K. J. F. Gaemers, Nucl. Phys. B132, 249 (1978).

[12]D. Drijard *et al.*, Phys. Lett. 81B, 250 (1979); K. L. Giboni *et al.*, *ibid.* 85B, 437 (1979); W. Lockman *et al.*, *ibid.* 85B, 443 (1979).

[13]V. L. Fitch *et al.*, Phys. Rev. Lett. 46, 761 (1981).

[14]C. Best, report of European Muon Collaboration data, XVI Rencontre de Moriond, 1981 (unpublished).